2-Deoxy-D-Glucose Ameliorates PKD Progression

Marco Chiaravalli,* Isaline Rowe,* Valeria Mannella,*† Giacomo Quilici,† Tamara Canu,‡ Veronica Bianchi,§ Antonia Gurgone,§ Sofia Antunes,‡ Patrizia D'Adamo,§ Antonio Esposito,‡ Giovanna Musco,† and Alessandra Boletta*

*Molecular Basis of Polycystic Kidney Disease Unit, †Biomolecular Nuclear Magnetic Resonance Unit, Division of Genetics and Cell Biology, ‡Center for Experimental Imaging, and §Division of Neuroscience, Istituto di Ricovero e Cura a Carattere Scientifico, San Raffaele Scientific Institute, Milan, Italy

ABSTRACT

Autosomal dominant polycystic kidney disease (ADPKD) is an important cause of ESRD for which there exists no approved therapy in the United States. Defective glucose metabolism has been identified as a feature of ADPKD, and inhibition of glycolysis using glucose analogs ameliorates aggressive PKD in preclinical models. Here, we investigated the effects of chronic treatment with low doses of the glucose analog 2-deoxy-D-glucose (2DG) on ADPKD progression in orthologous and slowly progressive murine models created by inducible inactivation of the *Pkd1* gene postnatally. As previously reported, early inactivation (postnatal days 11 and 12) of *Pkd1* resulted in PKD developing within weeks, whereas late inactivation (postnatal days 25–28) resulted in PKD developing in months. Irrespective of the timing of *Pkd1* gene inactivation, cystic kidneys showed enhanced uptake of ^{13}C-glucose and conversion to ^{13}C-lactate. Administration of 2DG restored normal renal levels of the phosphorylated forms of AMP–activated protein kinase and its target acetyl-CoA carboxylase. Furthermore, 2DG greatly retarded disease progression in both model systems, reducing the increase in total kidney volume and cystic index and markedly reducing CD45–positive cell infiltration. Notably, chronic administration of low doses (100 mg/kg 5 days per week) of 2DG did not result in any obvious sign of toxicity as assessed by analysis of brain and heart histology as well as behavioral tests. Our data provide proof of principle support for the use of 2DG as a therapeutic strategy in ADPKD.

J Am Soc Nephrol 27: 1958–1969, 2016. doi: 10.1681/ASN.2015030231

Autosomal dominant polycystic kidney disease (ADPKD) is the most common monogenic disorder affecting the kidney, with an estimated prevalence of individuals affected at birth of 1 in 500 to 1 in 1000.[1–3] The disease is caused by loss-of-function mutations in either *polycystic kidney disease 1* (*PKD1*; in 85% of patients) or *PKD2* (in the remaining 15%).[1–3] ADPKD is a chronic condition caused by the replacement of normal renal parenchyma by cysts, eventually causing complete loss of renal function in one half of the patients by the age of 50 years old.[1–4] In recent years, several cascades were found deregulated in the disease, leading to the identification of potential therapeutic targets in preclinical animal models.[1–3,5–7] Among all of these opportunities for therapy, the use of a vasopressin receptor antagonist, Tolvaptan, is the only one that so far resulted in an effective amelioration of disease progression in patients,[8–10] providing the first opportunity for therapy.[10] We and others have recently shown that metabolic alterations can be observed in animal models of PKD.[11–14] In particular, in a recent study, we have shown that defective glucose metabolism is a feature of ADPKD.[11] Both cells and kidneys carrying inactivation of the *Pkd1* gene were found to be addicted to glucose and generate most of their energy needs

Received March 2, 2015. Accepted September 3, 2015.

Published online ahead of print. Publication date available at www.jasn.org.

Correspondence: Dr. Alessandra Boletta, Division of Genetics and Cell Biology, Dibit, San Raffaele Scientific Institute, Via Olgettina 58, 20132 Milan, Italy. Email: boletta.alessandra@hsr.it

(ATP) through aerobic glycolysis in a process resembling the Warburg effect observed in cancer.[11] Furthermore, analysis of microarrays data generated from the cyst-lining epithelia in patients with ADPKD1 showed a clear signature of increase in the expression levels of genes involved in glycolysis and a significant decrease in genes involved in the opposite process, gluconeogenesis.[11,12] These data suggest that enhanced glycolytic rates might be present in the tissue from patients and that this metabolic alteration might be targeted for therapy.[11,12] Proof of concept studies on two distinct orthologous but very aggressive disease models showed that a glucose analog 2-deoxy-D-glucose (2DG) could, in principle, halt the progression of the disease.[11,12]

Here, we show that chronic administration of low doses of 2DG (100 mg/kg 5 days a week) has the ability to prevent disease progression in two slowly progressive, orthologous disease models in the presence of no obvious signs of toxicity. The results represent a proof of principle for this molecule to be used as a potential therapeutic approach in patients affected by ADPKD.

RESULTS

Enhanced Glycolysis in Two Slowly Progressive and Orthologous Models of PKD

To address whether chronic administration of low doses of 2DG remains effective, we used orthologous and slowly progressive disease models. Previous studies have shown that early inactivation of the *Pkd1* gene (before P13) results in an aggressive PKD model, whereas inactivation after P14 results in a slowly progressive disease model.[15,16] We intercrossed a Tamoxifen–inducible Cre line (*TmCre*)[17] with mice harboring floxable *Pkd1* alleles.[18] A single injection of Tamoxifen (10 mg/40 g) was performed at either P11 or P12, and the cystic kidneys were collected 2 weeks later (hereafter referred to as the medium-term model) (Figure 1A). In a second set of experiments, Tamoxifen was injected at P25–P28, and the kidneys were collected 3.5 months later (hereafter referred to as the long-term model) (Figure 1A). For simplicity, we refer to cystic mice ($Pkd1^{\Delta C/flox}TmCre$) or controls ($Pkd1^{flox/+}TmCre$; $Pkd1^{flox/+}$ and $Pkd1^{\Delta C/flox}$) interchangeably. Control animals were also injected with Tamoxifen at the indicated times and analyzed in parallel.

We first tested if the cystic kidneys generated on time-dependent inactivation of *Pkd1* result in an increase in glucose uptake as expected for highly glycolytic tissues and as we previously reported.[11] Injection of ^{13}C-glucose in either the medium– or the long–term animal model followed by analysis of kidney lysates by nuclear magnetic resonance (NMR) 40 minutes later revealed increased glucose uptake and increased conversion to ^{13}C-lactate in these tissues compared with control kidneys (Figure 1, B and C, Supplemental Figure 1A). On the basis of these results, we concluded that these animals should also be sensitive to the treatment with 2DG irrespective of the time of *Pkd1* inactivation. Next, we wondered whether treatment in the presence of 2DG would further increase glucose uptake as widely reported for cancers. Indeed, when 2DG (100 mg/kg) was administered to mice, we could observe a significant increase in the total amount of glucose (*i.e.*, glucose + 2DG) taken up by the kidney (Figure 1D). Since we previously reported an impairment in AMPK activation in the $Pkd1^{flox/-}KspCre$ mice, we wondered whether this molecule was altered in the slowly progressive PKD model as well. Indeed, we found that AMPK activity is reduced in the long–term mouse model (Figure 1E). Importantly, treatment with 2DG restored the activation state of AMPK (Figure 1E) but had no effect on the nuclear localization of pCREB, indicating that 2DG acts either on a different pathway or downstream of cAMP (Figure 1F).

2DG Effectively Retards Disease Progression in the Medium–Term PKD Model

Next, we tested the effect of treatment with 100 mg/kg 2DG for 5 days a week in the medium-term model. After 2 weeks of 2DG treatment, the kidneys appeared smaller than the vehicle-treated ones (Figure 2A), and the kidney to body weight ratio was significantly decreased compared with NaCl-treated animals (Figure 2B). Given that mice at this age are still growing, we tested whether treatment in the presence of 2DG might affect the growth curves of the animals, indicating some type of possible toxicity problem. We found that the total body weight of the animals was not affected by 2DG treatment in either control or PKD animals (Supplemental Figure 1B). Histologic analysis followed by quantification of the cystic index showed a marked reduction of the cystic burden in 2DG-treated animals compared with NaCl-treated ones, suggesting that the reduced kidney over body weight is indeed because of a marked decrease in the expansion of renal cysts (Figure 2, C and D).

2DG Effectively Retards Disease Progression in the Long–Term PKD Model

Next, we tested if late-onset PKD (the long-term model described in Figure 1A) could also be improved by the use of 100 mg/kg 2DG administered chronically for 5 days a week followed by a 2-day washout to minimize potential side effects. To follow the progression of the disease longitudinally in this long–term animal model, after the injection of Tamoxifen at P25, mice were followed up using *in vivo* magnetic resonance imaging (MRI); 30 days after injection of Tamoxifen, the first images of the kidneys were acquired (T=0), and the treatment was initiated immediately after (Figure 3A). Only litters containing at least two $Pkd1^{\Delta c/f}TmCre$ and one control were used for further analysis. Littermate mutant or control animals were treated with either 2DG (100 mg/kg 5 days a week) or vehicle only (NaCl); 55 (T=1M) or 85 (T=2M) days after inactivation (corresponding to 1 or 2 months of treatment), kidney volume was calculated by three-dimensional (3D) segmentation of *in vivo* MRI images (Figure 3, B and C), and

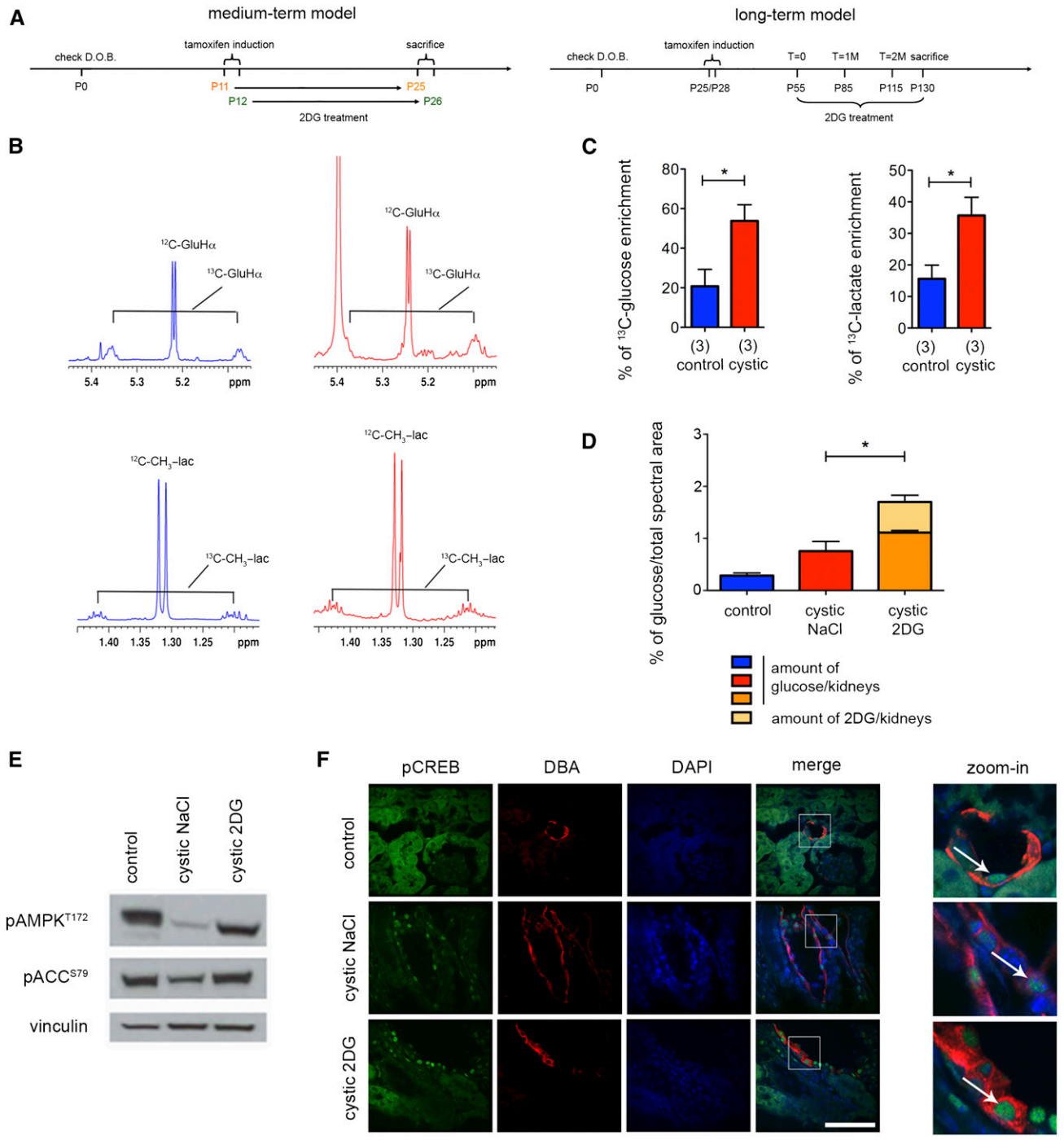

Figure 1. The Warburg effect the *Pkd1* inducible KO model irrespective of the inactivation timepoint and effects of 2DG. (A) Schematic view of the experimental plan. Medium-term model (left panel): *Pkd1*$^{\Delta C/flox}$*TmCre* mice were injected with a single dose of Tamoxifen (10 mg/40 g) at either P11 or P12, and kidneys were collected at P25 or P26, respectively. Long-term model (right panel): *Pkd1*$^{\Delta C/flox}$*TmCre* mice were injected with a single dose of Tamoxifen (10 mg/40 g) at P25–P28, MRI was performed after 1, 2, and 3 months, and kidneys were finally collected 2 weeks after the last MRI. (B and C) Comparison of ^{13}C enrichment on control and mutant mice. Representative ^{1}H-^{1}D spectra of the long-term experiment showing the ^{13}C satellite pattern of the ^{13}C-glucose (Hα) and ^{13}C-lactate (CβH3) in control (blue) and cystic mice (red) in the long-term model. The two sets of spectra were acquired with the same spectral parameters and normalized to dry weight, such that the peak intensity of individual resonances is directly comparable. (C) The percentage of ^{13}C-glucose and ^{13}C-lactate enrichment (calculated as described in Concise Methods) was higher in the kidneys from the cystic mice (*Pkd1*$^{\Delta C/flox}$*TmCre*) compared with those in the controls (*Pkd1*$^{flox/+}$*TmCre*; *Pkd1*$^{flox/+}$ and *Pkd1*$^{\Delta C/flox}$ interchangeably) as calculated from multiple samples acquired as in B. (D) The percentage of the total amount of glucose (glucose and 2DG) taken up by the kidneys of mice treated with 2DG (100 mg/kg) was

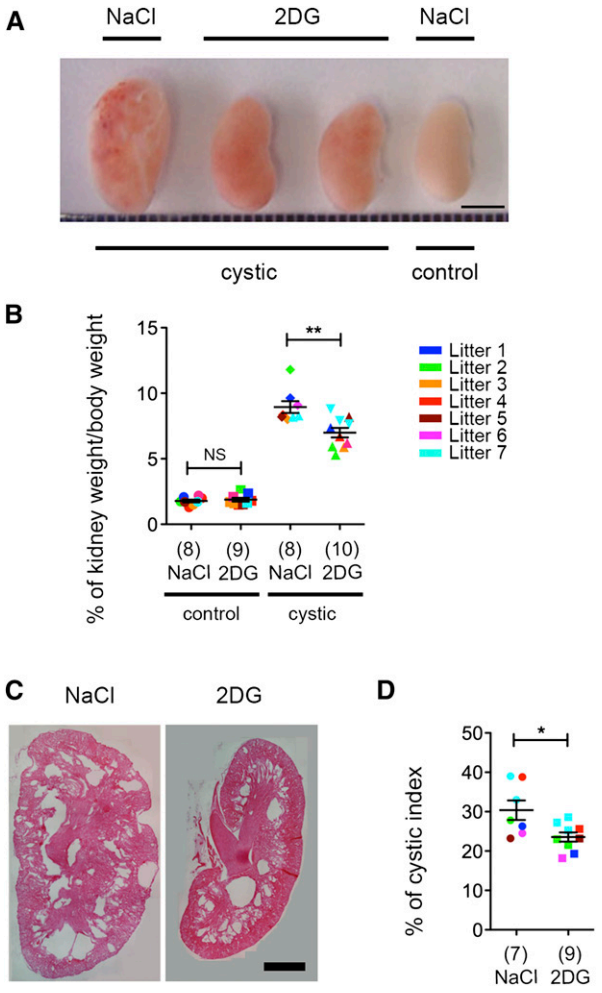

Figure 2. Treatment with 2DG ameliorates cystic kidney disease in the medium-term model. (A) Images of cystic kidneys treated with 2DG at 100 mg/kg or NaCl from P12 to P26 and littermates controls. The best example is shown (litter 2). (B) The percentage of kidney weight to total body weight in cystic mice treated as described in A was significantly reduced compared with the vehicle control (NaCl). The same treatment had no effect on the percentage of kidney to total body weight in control mice. The power of the study was 0.94. (C) Representative images of the histologic analysis of kidneys treated as described in A. (D) Cystic index calculated for the kidneys from *Pkd1*$^{\Delta C/flox}$*TmCre* mice treated with 2DG or vehicle as described in A–C. Means±SEMs are indicated. NS indicates $P \geq 0.05$. Scale bars, 4 mm in A; 1 mm in C. *$P<0.05$ determined using the Mann–Whitney test for B and D; **$P<0.01$ determined using the Mann–Whitney test for B and D.

blood was withdrawn from the tail. Notably, in this long-term model, we chose to initiate the 2DG treatment when the kidneys were already cystic and enlarged in size (Figure 3, A–C, Supplemental Table 1), but their function was not yet compromised, reasoning that this would be the condition in which patients affected by ADPKD would start therapy.

Despite the fact that the therapy was initiated when the kidneys were already enlarged and grossly cystic, monitoring showed a marked reduction in the increase of total kidney volume (TKV) of animals treated with 2DG compared with NaCl at both 1 and 2 months after treatment (Figure 3, A–C, Supplemental Table 1). Analysis of BUN at the different time points revealed that the functionality of the kidneys in this animal model is maintained for a relatively long period of time when the kidneys appear morphologically compromised, similar to what seems to occur in patients (Figure 3, C and D).[1] Importantly, 2DG–treated PKD animals tend to have a better preservation of renal function compared with vehicle-treated animals (Figure 3D), although we observed a more pronounced improvement in the TKV than in the renal function (Figure 3, C and D).

Two weeks after the last MRI, mice were euthanized and analyzed. The kidneys derived from 2DG-treated animals appeared much smaller than those extracted from vehicle-treated animals (Figure 3E), and in line with the MRI data, kidney over body weight of 2DG-treated animals was significantly reduced compared with that of mice treated with vehicle only (Figure 3, E and F). Of interest, we observed that there is a good linear correlation between the TKV and the kidney over body weight parameter in these animals (r^2=0.95) (Figure 3G).

2DG Improves the Cystic Index and Inflammatory Response in the Long–Term PKD Model in the Absence of Obvious Signs of Toxicity

Furthermore, histologic analysis revealed a significant reduction in cystic index in 2DG-treated mice compared with NaCl-treated ones (Figure 4, A and B, Supplemental Figure 1C). Importantly, we used real-time PCR for CD15 (granulocytes), CD68 (macrophages), and CD45 (leukocyte common antigen) to evaluate the infiltration in these kidneys. We noticed a very prominent infiltration rate in the cystic tissues for all of these three markers, in line with previous studies.[19] Of interest, 2DG significantly reduced the levels of CD45-expressing cells as assayed both by RT-PCR and immunohistochemistry (Figure 4, C and D). The reduced infiltration rates might reflect a reduced tissue damage in the long–term PKD model. Alternatively, these results might suggest that 2DG counteracts tissue infiltration in addition to slowing down cystic epithelia proliferation.

In a previous study, we showed that 2DG limits the expansion of cysts specifically induced in the distal tubule/collecting ducts by a KspCre line.[11] In this model, we observe the presence of cysts of different origin, as previously reported

significantly increased. (E) pAMPK T172 and its target pAcetyl-CoA Carboxylase (pACC) S69 were downregulated in cystic kidneys treated with vehicle compared with control and restored after 2DG treatment. (F) Nuclear pCREB staining is observed in the DBA-positive cysts in both 2DG–treated and untreated cystic kidneys. Scale bar, 50 μm in F. *$P<0.05$ determined using the unpaired t-test. D.O.B., day of birth.

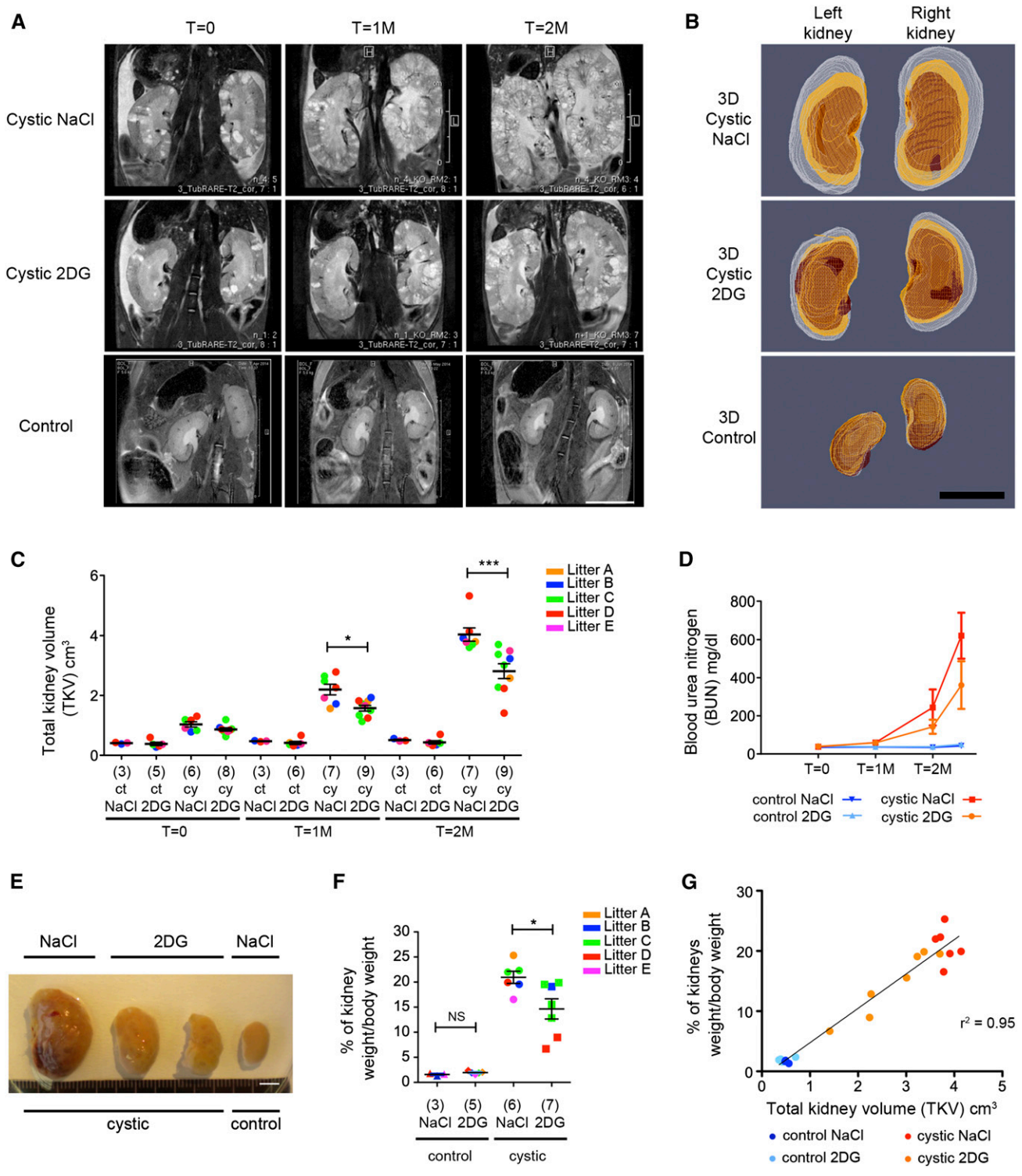

Figure 3. Treatment with 2DG retards PKD progression in the long-term model. (A) Follow-up of kidneys *in vivo* using MRI in the long–term animal model. Both cystic (*Pkd1*$^{\Delta C/flox}$*TmCre*) and control (*Pkd1*$^{flox/+}$*TmCre*; *Pkd1*$^{flox/+}$ and *Pkd1*$^{\Delta C/flox}$ interchangeably) animals were injected with a single dose of Tamoxifen (10 mg/40 g) at P25/P28 followed by treatment with either vehicle (NaCl) or 2DG at 100 mg/kg. Representative images acquired by MRI as described in Concise Methods are shown. The first MRI was acquired 1 month after injection of Tamoxifen before initiation of treatment (*T*=0), and the second and third MRIs were acquired 1 (*T*=1M) and 2 (*T*=2M) months later, respectively. (B) Three-dimensional reconstruction of the kidneys from the left and right kidneys 1 (red), 2 (orange), and 3 months (white) after injection. (C) TKV was calculated for the cystic and control kidneys treated with 100 mg/kg 2DG or vehicle only at each of the time points described in A. The volume of the 2DG–treated cystic kidneys is significantly reduced both 1 and 2 months after

(Supplemental Figure 1D). Of interest, treatment with 2DG did not change the percentage of cysts of different origin, suggesting that the molecule is equally active on cysts of every tubular segment (Supplemental Figure 1D). Thus, we used Lotus Tetragonolobus Lectin (LTL; VECTOR) staining to test if cysts of proximal tubule origin also respond to 2DG treatment. Indeed, LTL-positive cysts are smaller in volume on 2DG treatment compared with NaCl-treated kidneys (NaCl: $3.2\times10^3\pm0.5\times10^3$ μm^2, n=48; 2DG: $2.8\times10^3\pm0.3\times10^3$ μm^2; mean±SEM; n=160 from three different litters), suggesting that 2DG effectively retards cyst expansion in both the distal and collecting ducts and the proximal tubules.

Importantly, 2DG treatment had no significant effect on the total body weight in either controls or PKD animals (Figure 4E). Notably, additional biochemical parameters, including liver toxicity markers (alanine amino transferase, aspartate aminotransferase, and alkaline phosphatase), revealed that no obvious sign of toxicity could be appreciated (Figure 4, F and G, Supplemental Figure 1E). These results are in line with previous reports describing that low doses of 2DG administered chronically in animal models are well tolerated and do not cause toxicity.[20,21] However, one study has reported signs of toxicity in the heart when high doses of 2DG are ingested by the rat.[22] Thus, we designed a study similar to the one conducted in the cystic animals on wild-type mice with the aim of testing the toxicity of this compound in our conditions (*i.e.*, intraperitoneal administration of 100 mg/kg 5 days a week for 2.5 months). In these animals, we did not observe any major sign of kidney toxicity (measured as BUN), liver toxicity (measured as alanine amino transferase, aspartate aminotransferase, lactate dehydrogenase, and albumin), or heart toxicity (CK) (Supplemental Table 2). In these animals, we also observed no difference in body weight, food and water intake, or body temperature (Supplemental Figure 2) as well as the levels of circulating glucose and insulin (Supplemental Figure 3, A and B). In particular, we focused our attention on tissues highly depending on glucose, such as heart and brain, to determine whether they might be affected by our treatment regimen. These animals were subjected to behavioral tests followed by histologic analysis. First, mice were subjected to the flag-visible version of the water maze test to assess visual ability in 2DG–treated wild–type mice (n=8) and nontreated mice (n=6). Both groups had normal visual ability (ANOVA repeated measures for treatment effect on the time to reach the flagged platform F[1,12]=0.11; P=0.74). Second, mice were subjected to the standard hidden platform version of the water maze.[23] Of great interest, the 2DG-treated mice were more efficient in the time to reach the platform during the trials (Figure 4H) (ANOVA repeated measures for escape latency F[1,12]=8.8; P=0.01 with no interaction between treatment× days F[1,14]=1.05; P=0.40), which was also shown by the significant difference in the pathway to reach the platform (Supplemental Figure 3C). No differences between the two groups during probe trial in crossing the former goal annulus could be observed (Figure 4I) (ANOVA repeated measures for annulus crossing F[1,12]=0.18; P=0.68). Third, mice were subjected to the spontaneous alternation test to assess working memory. 2DG treatment has no effect on working memory (Supplemental Figure 3, E and F). These results suggest that 2DG administration tends to improve spatial memory acquisition but has no effect on the working memory. These data are of great interest and will require further investigation. Importantly, all other parameters analyzed, including motility scored by speed of movement, were not affected by 2DG (Supplemental Figure 3D). At the completion of the experiment, animals were euthanized and analyzed at the histologic level. Hearts did not appear to be grossly altered at the histologic level in these animals, and no vacuolization could be observed (Figure 4J). Similarly, histologic analysis of brains did not reveal any major problem (Figure 4J). Quantification of the hippocampal region and cortical thickness normalized by the total brain area did not reveal morphologic alterations (NaCl hip mean, 0.052 μm^2 ±SEM [0.002]; 2DG hip mean, 0.050 μm^2 ±SEM [0.004]; NaCl cortical thickness, 893.4 μm ±SEM [48.5]; 2DG cortical thickness, 904.5 μm ±SEM [118.8]).

DISCUSSION

Our study shows that 2DG effectively slows down disease progression in orthologous and mild PKD mice models and that it does so irrespective of the window of time in which the *Pkd1* gene is inactivated. These results suggest that inhibition of glycolysis in ADPKD might be effective in early as well as late disease manifestations. Furthermore, our data show that 2DG at low doses has no obvious toxicity effects even on chronic administration, in line with previous studies.[20,21] However, some controversies on the effects of 2DG administration have been reported in the literature. Chronic ingestion for 6 months of high doses of 2DG (250 mg/kg per day) were reported to cause mortality and heart vacuolization in the rat.[22] On the contrary, a second study reported that chronic

treatment. The power of the study was 0.93. (D) BUN was evaluated on the blood withdrawn from the tails of the animals at each time point in which MRIs were acquired plus at euthanasia 2 weeks after the last MRI, showing a trend to renal function improvement in cystic animals on 2DG treatment compared with vehicle–treated (NaCl) cystic animals. (E) Images of cystic and control kidneys treated as described above and collected 2 weeks after the last MRI show a significant reduction of volume after 2DG treatment. The best example is shown. (F) Percentage of kidney weight to total body weight in the cystic or control mice treated as described above. (G) Graph showing the relation between the kidney to total body weight versus the TKV evaluated by MRI shows a linear correlation (r^2=0.95). NS indicates $P\geq0.05$. Scale bars, 1 cm in A and B; 5 mm in E. *$P<0.05$ determined using the Mann–Whitney test for C and F; ***$P<0.001$ determined using the Mann–Whitney test for C and F.

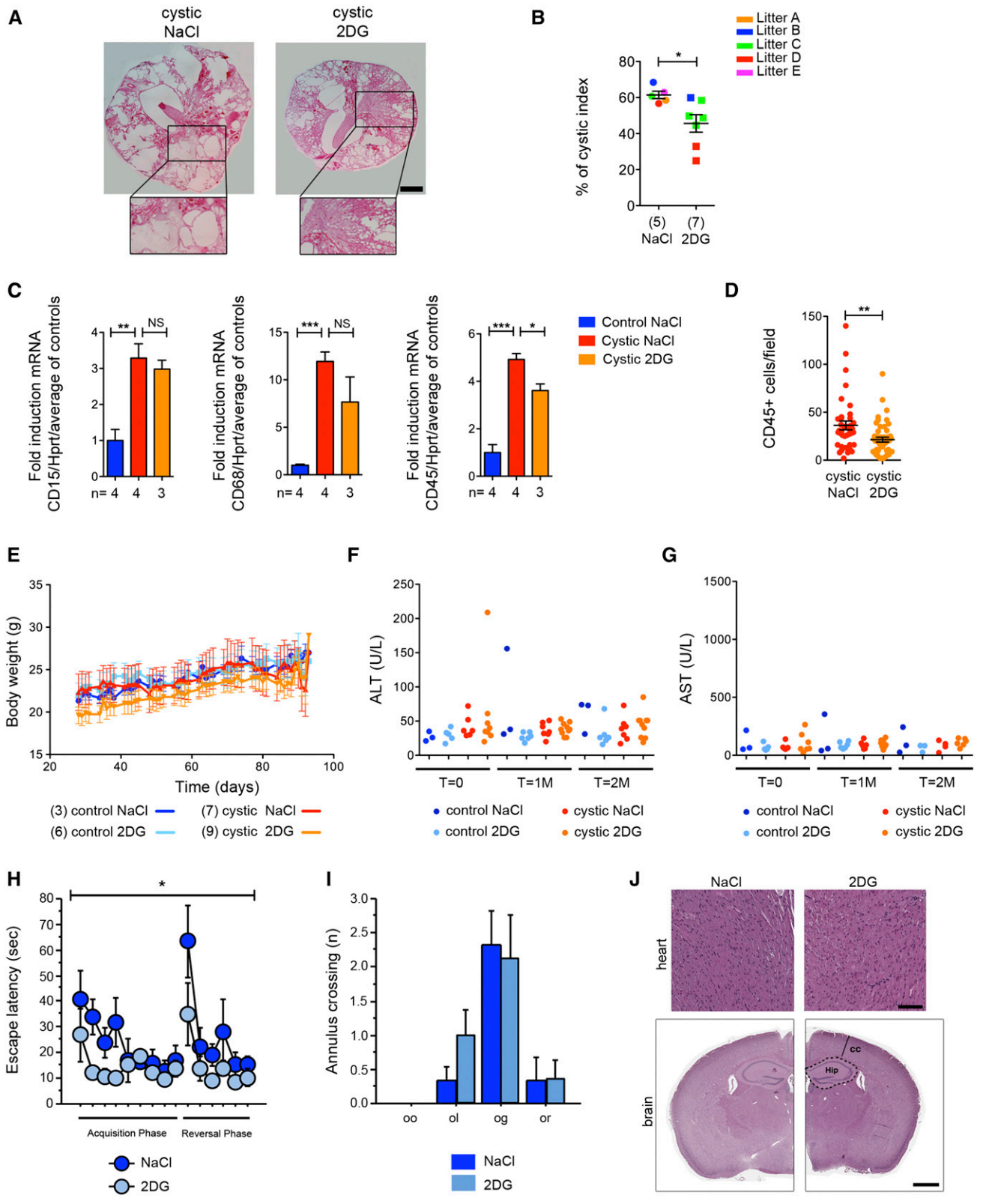

Figure 4. Treatment with 2DG ameliorates cystic kidney disease in the long-term model without evident signs of toxicity. (A) Representative histologic pictures of treated cystic (*Pkd1*$^{\Delta C/flox}$*TmCre*) kidneys as defined in Figure 1A with 2DG or vehicle (NaCl) only reveal a marked reduction in cystic burden in the 2DG-treated kidneys. (B) Cystic index evaluated in kidneys from cystic (*Pkd1*$^{\Delta C/flox}$*TmCre*) animals treated with either 2DG or vehicle (NaCl) only as described in A. (C) Key inflammation genes were upregulated in untreated

intraperitoneal injections of even higher doses (500 mg/kg per day) did not cause major toxicity in the rat.[20] In this study, we show that low doses of 2DG (100 mg/kg) injected intraperitoneally for 5 days a week followed by 2 days of washout for 2.5 months did not cause any apparent sign of toxicity. Although the route of administration might be the reason for these discrepancies, in light of the studies in rats, some caution should be used, and additional long–term studies should be pursued to establish the possible toxicity of this compound and the optimal route of administration. Importantly, our study indicates that the beneficial effects seem more prominent in the long–term, chronically treated PKD model, even if 2DG administration was initiated in cystic and grossly enlarged kidneys. Because this resembles the stage of ADPKD in which patients are selected for a potential intervention, we speculate that 2DG would be effective in retarding disease progression in humans as well, where increased lactate accumulation has been reported, further suggesting that defective glycolysis is likely to be present in patients.[11,24] Importantly, 2DG proved effective in retarding cyst expansion in both distal tubules and collecting ducts and cysts of proximal tubule origin.

In conclusion, the efficacy, low toxicity, and capability to reduce the expansion of cysts of all origins make 2DG a good candidate for further testing in humans affected by ADPKD. This molecule is well tolerated[25,26] and might offer important advantages over molecules such as Tolvaptan, which has action that is limited to cysts originating from specific segments of the nephron (distal tubules and collecting ducts).[10] Furthermore, we speculate that 2DG might be active in cysts originating in other organs, such as the bile ducts in the liver or pancreatic cysts, because glucose transporters are ubiquitous. With respect to this, it will be interesting to test if enhanced glycolysis is a feature of these cysts as well.

Despite the potential advantages listed above, it should be considered that 2DG is not currently approved for any human condition, and additional toxicity studies on long administration should be performed. Finally, the fact that 2DG seems to restore pAMPK levels but not the nuclear localization of pCREB suggests that enhanced glycolysis is either a parallel pathway or activated downstream of cAMP. It will be important to perform additional studies to distinguish between these two possibilities, because these data might indicate that combination therapy between Tolvaptan and 2DG might offer an additional opportunity to achieve a further beneficial effect.

CONCISE METHODS

Mouse Lines

We crossed C57/BL6 *Pkd1*$^{\Delta C/+}$ mice[18] to TmCre B6.Cg-Tg(CAG-cre/Esr1*)5Amc/J mice (stock 004682; Jackson Laboratories). The progeny C57/BL6 TmCre *Pkd1*$^{\Delta C/+}$ was bred with C57/BL6 *Pkd1*$^{flox/flox}$ mice to produce the mice used in these studies. Cre recombinase activity was induced by a single injection of Tamoxifen at P11 or P12 for the medium-term model or P25/P28 for the long-term model. Tamoxifen (catalog no. T5648; 10 mg/40 g; Sigma-Aldrich) freshly prepared and dissolved in corn oil (catalog no. C8267; Sigma-Aldrich) by continuous shaking at 37°C for 4 hours was injected intraperitoneally. For all animal care and experimental protocols, a specific protocol was approved (IACUC 548) by the Institutional Care and Use Ethical Committee at the San Raffaele Scientific Institute and further approved by the Italian Ministry of Health. For all animal work, the female to male ratio was 1:1, and mice were randomized for each experiment.

2DG Treatment

For treatments, mice were injected intraperitoneally with 2DG (catalog no. D6134; Sigma-Aldrich) or vehicle (NaCl) once daily for 5 consecutive days a week from P12 to P27 for the medium term and from P25/P28 to P130 for the long term at 100 mg/kg body wt. For the long-term model, five different litters were used (Supplemental Table 1).

Statistical Analyses

We calculated the statistical significance of differences using Mann–Whitney or unpaired *t* test using GraphPad Prism (version 5.0). For calculation of the power of the studies, for the medium-term animals,

cystic (*Pkd1*$^{\Delta C/flox}$*TmCre*) compared with control kidneys. With 2DG, a trend of reduction (CD15 and CD68) or significant reduction (CD45) could be observed. Hprt expression was used as a normalizer for total cell number. (D) Immunohistochemistry confirmed a significant reduction in the number of CD45-positive cells per acquired field (350×435 μm) in 2DG–treated cystic kidneys compared with NaCl-treated tissues; ten fields were acquired in one renal medial section from three different animals. (E) 2DG treatment had no significant effect on the total body weight in either controls or mutant mice. (F) Alanine aminotransferase (ALT) and (G) aspartate aminotransferase (AST) values showed no liver toxicity induced by 2DG in any of the animals used. (H) During the standard hidden platform version of the water maze trials, 2DG-treated mice were faster to reach the hidden platform (escape latency) compared with the vehicle-treated littermates. (I) No difference was observed in the annulus crossing during the probe trial in the first day (first 30 seconds) of the reversal phase. Old goal (og) indicates the old platform position, old opposite (oo) specifies the new opposite position of the platform, and old left (ol) and old right (or) show the quadrant at the left and the right of the old goal, respectively. (J) Representative images of heart sections of NaCl- (n=6) and 2DG-treated (n=9) mice stained with Hematoxylin-Eosin showing absence of vacuolization caused by 2DG (upper panel). Representative brain coronal sections (5 μm) of NaCl (n=5) and 2DG-treated (n=6) mice stained with Hematoxylin-Eosin show absence of differences (lower panel). Cortical thickness (CC) and the hippocampal region (Hip) are indicated. NS indicates $P \geq 0.05$. Scale bars, 100 μm in J, upper panel; 1 mm in J, lower panel. *$P<0.05$ determined using the Mann–Whitney test for B and D, *t* test for C, and ANOVA for H and I; **$P<0.01$ determined using the Mann–Whitney test for B and D, *t* test for C, and ANOVA for H and I; ***$P<0.001$ determined using the Mann–Whitney test for B and D, *t* test for C, and ANOVA for H and I.

we used as an end point, kidney/body weight. For this study, the sample sizes were eight (for the NaCl-treated mice) and ten (for the 2DG-treated mice). These groups achieve 94% power (0.94) to detect a difference of 2.10 between the null hypothesis that both group means are 8.90 (NaCl) and the alternative hypothesis that the mean of group 2 is 6.80 (2DG), with known group SDs of 1.27 and 1.02, respectively, and a significance level (α) of 0.05000 using a two–sided Mann–Whitney test assuming that the actual distribution is normal.

For the long-term study, we used TKVs at 2 months of treatment as an end point. Group sample sizes of seven (NaCl) and nine (2DG) achieve 93% power to detect a difference of 1.23 between the null hypothesis that both group means are 4.04 and the alternative hypothesis that the mean of group 2 is 2.81, with known group SDs of 0.59 and 0.74, respectively, and a significance level (α) of 0.05000 using a two–sided Mann–Whitney test assuming that the actual distribution is normal. For behavioral studies, ANOVA with repeated measures was used for statistical analysis (StatView; SAS Institute, Cary, NC).

NMR Acquisition and Data Analyses

P20 and P130 mutant mice (*Pkd1*$^{\Delta C/flox}$*TmCre* induced with Tamoxifen at P12 and P25/P28, respectively) and the control littermates (*Pkd1*$^{flox/+}$*TmCre* and *Pkd1*$^{flox/+}$) were starved for 5–10 hours and then injected intraperitoneally with 1000 mg/kg body wt ^{13}C uniformly labeled glucose (catalog no. CC850P10; Cortecnet); 40 minutes after the injection, the mice were euthanized, and their kidneys were weighted, immediately frozen in liquid nitrogen, and lyophilized for 24 hours. After lyophylization, kidneys were weighted again to obtain their dry weights. Polar metabolites were extracted from tissues using classic MeOH/$CHCl_3$ solvent extraction strategy.[27] Polar phases were lyophilized for 24 hours and subsequently resuspended in 150 mM phosphate buffer with the addition of 100 μM DSS as internal chemical shift reference and sodium azide (0.02%) for sample preservation. Final volumes were 250 μl with D_2O (100%).

NMR spectra were recorded at 25°C on a Bruker Avance 600 Ultra Shield TM Plus 600-MHz Spectrometer equipped with triple-resonance cryoprobe and pulsed field gradients. ^{1}H-^{1}D NMR spectra (noesypr1d) were recorded with an acquisition time of 2 seconds, a recycle time of 6 seconds to minimize peak saturation, and 256 and 1024 transients for long- and medium-term mice, respectively. ^{1}H-^{1}D NMR spectra were typically processed with zero filling to 131,000 points and apodized with an unshifted Gaussian and a 0.5-Hz line broadening exponential. The spectra were carefully phased and baseplane corrected before peak integration.

The global spectrum deconvolution algorithm implemented in the Mnova9.0 software package of Mestrelab was used to deconvolve and integrate the spectra.[28]

To confirm glucose and ^{13}C positional isotopomers, 2D-^{1}H TOCSY and ^{1}H-^{13}C HSQC experiments were also acquired. TOCSY spectra were acquired with a standard pulse sequence with a mixing time of 60 ms, 512 increments, and 40 or 56 transients for long- and medium-term mice, respectively; 2D ^{1}H-^{13}C HSQC spectra were acquired with a total of three transients for each of 400 increments. Spectral widths were set to 12 and 185 ppm for ^{1}H and ^{13}C, respectively (offsets at 4.7 and 75 ppm, respectively).

The ^{13}C enrichment of glucose was determined integrating and deconvolving the appropriate ^{1}H^{13}C satellites (at 5.36 and 5.08 ppm) and the ^{1}H^{12}C peak (5.25 ppm), corresponding to the Hα anomeric proton in the 1D-^{1}H NMR spectra. Lactate^{13}C enrichment was determined considering the ^{1}H^{13}C satellites (at 1.42 and 1.22 ppm) and the ^{1}H^{12}C peak at 1.31 ppm, corresponding to the methyl proton of lactate in the ^{1}H-^{1}D NMR spectra. The percentage of ^{13}C abundance of labeled metabolites was calculated from the ratio of the peak areas of the satellite peaks to the total peak intensity according to the equation $F=I_{13C\_satellites}/I_{13C\_satellites}+I_{12C\_central\ peak}$, where I is the peak area.[29,30] We observed that the satellite at 5.36 ppm was often difficult to deconvolve because of partial overlap with the allantoin peak; its integral value was, therefore, obtained from the symmetric satellite peak at 5.08 ppm.

MRI

All MRI studies were performed on a 7-T Preclinical Scanner (BioSpec 70/30 USR, Paravision 5.1; Bruker) equipped with 450/675 mT/m gradients (slew rate: 3400–4500 T/m per second; rise time: 140 μs) and a circular polarized mouse body volume coil with an inner diameter of 40 mm. Mice were under general anesthesia obtained by 1.5%–2% isoflurane vaporized in 100% oxygen (flow of 1 L/min). Breathing and body temperature were monitored during MRI (SA Instruments, Inc., Stony Brook, NY) and maintained around 30 breaths per minute and 37°C, respectively.

All MRI studies included axial and coronal RARE T2–weighted sequences (slice thickness, 0.6 mm; interslice gap, 0 mm) with a number of slices, allowing a complete coverage of both kidneys.

Manual segmentation of the kidneys was performed on each slice, excluding the collecting system and kidney volume results from automatic summation of voxel volumes (OsiriX, version 5.6, 32 bit; Pixmeo SARL). Five litters were used (A–E), including three control mice treated with vehicle, six control mice treated with 2DG, seven cystic mice treated with vehicle, and nine cystic mice treated with 2DG. Both acquisition and analysis of the data were performed blindly by an operator unaware of genotype or treatment conditions. The data generated by analysis of all animals used in the study are included in Supplemental Table 1. For 3D reconstruction, the kidneys were manually segmented on each MRI slice using Mipav (Centre for Information Technology, National Institutes of Health, Bethesda, MD), and correspondent 3D surfaces were generated and visualized using Paraview (Kitware, Inc., New York, NY). Each kidney surface was aligned to the first MRI time point on the basis of the renal pelvis location.

Clinical Chemistry

Analysis of serum samples was assessed by ILab Aries, a bench-top analyzer that can perform photometry, turbidimetry, and potentiometry tests (Instrumentation Laboratory, Werfen Group, Milan, Italy). All parameters were detected using kits and controls supplied by ILab Aries. Standard controls were run before each determination to monitor the precision throughout the experiment, and the values obtained for controls were always within the expected ranges.

Histology

After euthanasia, kidneys were washed in PBS, weighed, and fixed in 4% paraformaldehyde (catalog no. P6148; Sigma-Aldrich). After incubation in a sucrose in PBS gradient scale from 10% to 30%, samples were incubated in 10% glycerol (catalog no. G5150; Sigma-Aldrich) in a mixture of optimal cutting temperature medium (Killik; catalog no. 05–9801; BIO-OPTICA) and 30% sucrose and then embedded in OCT. Cryostat sections were air dried for 1 hour, rehydrated in PBS, incubated in 1:10 Harris Hematoxylin (catalog no. HHS16; Sigma-Aldrich) for 2 minutes, washed, and incubated in Eosin Y (catalog no. 05–10002/L; BIO-OPTICA) for 7 minutes. Sections were finally washed again, dehydrated, and mounted in DPX Mountant (catalog no. 44581; Sigma-Aldrich) for histology.

For brain and heart histology, organs were harvested directly after euthanasia in zinc-formalin and transferred into 70% ethanol 24 hours later. Tissues were then processed, embedded in paraffin, and stained; sections (5 mm) were dewaxed, hydrated through a graded decrease alcohol series, and stained for Hematoxylin-Eosin (BIO-OPTICA). Bright-field images were acquired through an Aperio Scanscope System AT2 Microscope and an ImageScope program (Leica Biosystem) following the manufacturer's instructions. For quantifications of the brain histology, four slices for each mouse were analyzed from Bregma −1.225 mm to Bregma −2.55 mm. Cortical area was analyzed at ×2.5 enlargement, and the hippocampal area and the cortical thickness were analyzed at ×5 enlargement. The software used for the analyses was Aperio ImageScope v12.1.0.5029 (Leica Biosystem). Statistical analyses were made with GraphPad Prism (version 5.0).

Cystic Index

Images of longitudinal sections from the inner part of the kidney after Hematoxylin-Eosin staining were taken (Nikon Eclipse E600 Microscope, Nikon Digital Camera DXM1200, and ACT-1 software). The ImageJ program (http://rsb.info.nih.gov/ij/) was then used to quantify the total surface of the kidney and the total cystic area using 5000 μm^2 as a cutoff to include a cyst. We next calculated the ratio between the cystic area and the total area of the kidney.

Antibodies Lectins

Anti–pAcetyl-CoA Carboxylase (Ser79) 07–303 at 1:1000, anti-pAMPK (Thr172) 40H9 2535 at 1:1000, anti-pCREB (Ser133; 87G3) 9198 at 1:400 were from Cell Signaling Technology. Antivinculin 05–386 (clone V284) was from Millipore at 1:10,000. Lectin Dolichos Biflorus Agglutinin (DBA) (VECTOR) and LTL were used at 1:100.

LTL/DBA Staining

Kidneys were harvested, fixed, and cut as described above for histology. Sections were rehydrated; permeabilized with 0.1% PBS-Triton X-100; blocked with PBS, 3% BSA, and 5% normal goat serum for 1 hour; and incubated overnight with Lectin DBA and LTL diluted at 1:100. After washing with PBS, sections were mounted with Mowiol with 4′,6-Diamidine-2′-phenylindole dihydrochloride (DAPI). At least five pictures of sections of each kidney from mice of four litters (four kidneys treated with 2DG and four kidneys treated with NaCl) were obtained using an Axiophot Microscope (Carl Zeiss), and the area of each cyst was quantified using ImageJ software.

Western Blot Analysis

For Western blot analysis, kidneys were smashed on dry ice and resuspended in lysis buffer (10 mM Hepes, 10 mM KCl, 1.5 mM $MgCl_2$, 0.34 M sucrose, 1 mM dithiothreitol, 10% glycerol [pH 7.9], 0.1% Triton X-100, complete protease inhibitors [Roche], and phosphatase inhibitors; 1 mM final concentration of glycerophosphate, sodium orthovanadate, and sodium fluoride). After centrifugation, we separated the supernatant and the pellet. The supernatant was clarified by a second centrifugation. We resolved proteins in an SDS-PAGE gel and transferred them onto polyvinylidene fluoride membranes. Next, we used 5% milk in Tris-buffered saline and Tween 20 for blocking and secondary antibody incubations, and 3% BSA in Tris-buffered saline and Tween 20 was used for incubations with primary antibodies. We visualized horseradish peroxidase (HRP) –conjugated secondary antibodies (anti-rabbit HRP linked [NA934V] 1:10,000 and anti-mouse HRP linked [NXA931] 1:10,000; GE Healthcare) using the ECL System (Amersham).

Immunofluorescence

For immunofluorescence, kidneys were air dried for 30 minutes, washed in PBS, permeabilized in PBS and Triton X-100 (0.1%), blocked with 3% BSA in PBS, incubated overnight at 4°C with the antibody to CD45 or pCREB in blocking solution, washed, and incubated with the secondary antibody Alexa Fluor 488 anti-rat and anti-rabbit (A21441; Invitrogen) for 1 hour. For the p-CREB immunofluorescence, DBA was incubated together with the secondary antibody.

Real–Time PCR Analysis

We isolated total RNA from whole kidneys using the EuroGOLD TriFast Kit (Euroclone) and obtained cDNA using oligo(dT) primers (Invitrogen) and Superscript II Reverse Transcription (Invitrogen). We performed quantitative real–time PCR in duplicates using LightCycler480 (Roche Molecular Diagnostics) using SYBR Green I Master Mix.

The primers used were the following: mCD45: forward: 5-GAGGTGGGTGTGGATGAACT-3, reverse: 5-GTTGGATCGCTCCTGGAATA-3; mCD45: forward: 5-GGAGACCAGGAAGTCTGTGC-3, reverse: *5-GTTCTGGGCTCCTTCCTCTT-3*; mCD68: forward: *5-CTGACAAGGGACACTTCGGG-3*, reverse: *5-AGGCCAATGATGAGAGGCAG-3*; and Hprt: forward: *5-TTATGTCCCCCGTTGACTGA-3*, reverse: 5-ACATTGTGGCCCTCTGTGTG-3.

Water Maze Task and Spontaneous Alternation Test

Animals were maintained on a reversed 12-hour light/dark cycle at 22°C–24°C. Food and water were available *ad libitum* in the home cage. All behavioral procedures were approved by the Animal Care of the San Raffaele Scientific Institute and the National Ministry of Health (IACUC 653). All of the behavioral tests were assessed on 3-month-old mice comparing 2DG–treated and nontreated wild–type mice.

The hidden platform version of the water maze was used to test spatial reference memory.[23] Visual ability was tested in the flag-visible version for four consecutive trials in 1 day. Spontaneous alternation task was used to measure hippocampus–dependent spatial working memory in a nonfood-rewarded task. A mouse was released in the

central hub of a cross maze (four arms) and left free to explore for 10 minutes. Number and sequence of arm entries were recorded. A correct alternation was considered when no more than one repetition over five entries was made.

During all tests, animals were videotracked using the EthoVision 2.3 System (Noldus Information Technology, Wageningen, The Netherlands), with an image frequency of 4.2 per second. Raw data were transferred to Wintrack 2.4 for offline analysis.

ACKNOWLEDGMENTS

The authors thank the other members of the laboratories of G.M. and A.B. for helpful discussions; the Ospedale San Raffaele Mouse Clinic Intramural Project for technical support, particularly I. Fermo and M. Raso from the Clinical Chemistry and Hematology Murine Laboratory for hematologic analysis and A. Fiocchi for histologic analysis; Dr. G. Calori for help with the statistical analysis; and L. Rigamonti for help with immunologic studies. The authors also thank Dr. S. Bramani for continuous support.

This study was funded by the Italian Association for PKD (Associazione Italiana Rene Policistico; to M.C. and A.B.), Telethon Foundation Grant GGP12182, Italian Ministry of Health Grant RF-2011-02351840 (to G.M. and A.B.), and PKD Foundation Grant 187G14a (to A.B.).

DISCLOSURES

M.C., I.R., and A.B. are coinventors on a patent for the use of glycolysis inhibitors in PKD.

REFERENCES

1. Torres VE, Harris PC, Pirson Y: Autosomal dominant polycystic kidney disease. *Lancet* 369: 1287–1301, 2007
2. Harris PC, Torres VE: Polycystic kidney disease. *Annu Rev Med* 60: 321–337, 2009
3. Boletta A: Emerging evidence of a link between the polycystins and the mTOR pathways. *PathoGenetics* 2: 6, 2009
4. Grantham JJ, Geiser JL, Evan AP: Cyst formation and growth in autosomal dominant polycystic kidney disease. *Kidney Int* 31: 1145–1152, 1987
5. Gattone VH 2nd, Wang X, Harris PC, Torres VE: Inhibition of renal cystic disease development and progression by a vasopressin V2 receptor antagonist. *Nat Med* 9: 1323–1326, 2003
6. Shillingford JM, Murcia NS, Larson CH, Low SH, Hedgepeth R, Brown N, Flask CA, Novick AC, Goldfarb DA, Kramer-Zucker A, Walz G, Piontek KB, Germino GG, Weimbs T: The mTOR pathway is regulated by polycystin-1, and its inhibition reverses renal cystogenesis in polycystic kidney disease. *Proc Natl Acad Sci U S A* 103: 5466–5471, 2006
7. Yamaguchi T, Wallace DP, Magenheimer BS, Hempson SJ, Grantham JJ, Calvet JP: Calcium restriction allows cAMP activation of the B-Raf/ERK pathway, switching cells to a cAMP-dependent growth-stimulated phenotype. *J Biol Chem* 279: 40419–40430, 2004
8. Walz G, Budde K, Mannaa M, Nürnberger J, Wanner C, Sommerer C, Kunzendorf U, Banas B, Hörl WH, Obermüller N, Arns W, Pavenstädt H, Gaedeke J, Büchert M, May C, Gschaidmeier H, Kramer S, Eckardt KU: Everolimus in patients with autosomal dominant polycystic kidney disease. *N Engl J Med* 363: 830–840, 2010
9. Serra AL, Poster D, Kistler AD, Krauer F, Raina S, Young J, Rentsch KM, Spanaus KS, Senn O, Kristanto P, Scheffel H, Weishaupt D, Wüthrich RP: Sirolimus and kidney growth in autosomal dominant polycystic kidney disease. *N Engl J Med* 363: 820–829, 2010
10. Torres VE, Chapman AB, Devuyst O, Gansevoort RT, Grantham JJ, Higashihara E, Perrone RD, Krasa HB, Ouyang J, Czerwiec FS; TEMPO 3:4 Trial Investigators: Tolvaptan in patients with autosomal dominant polycystic kidney disease. *N Engl J Med* 367: 2407–2418, 2012
11. Rowe I, Chiaravalli M, Mannella V, Ulisse V, Quilici G, Pema M, Song XW, Xu H, Mari S, Qian F, Pei Y, Musco G, Boletta A: Defective glucose metabolism in polycystic kidney disease identifies a new therapeutic strategy. *Nat Med* 19: 488–493, 2013
12. Rowe I, Boletta A: Defective metabolism in polycystic kidney disease: Potential for therapy and open questions. *Nephrol Dial Transplant* 29: 1480–1486, 2014
13. Priolo C, Henske EP: Metabolic reprogramming in polycystic kidney disease. *Nat Med* 19: 407–409, 2013
14. Menezes LF, Zhou F, Patterson AD, Piontek KB, Krausz KW, Gonzalez FJ, Germino GG: Network analysis of a Pkd1-mouse model of autosomal dominant polycystic kidney disease identifies HNF4α as a disease modifier. *PLoS Genet* 8: e1003053, 2012
15. Lantinga-van Leeuwen IS, Leonhard WN, van der Wal A, Breuning MH, de Heer E, Peters DJ: Kidney-specific inactivation of the Pkd1 gene induces rapid cyst formation in developing kidneys and a slow onset of disease in adult mice. *Hum Mol Genet* 16: 3188–3196, 2007
16. Piontek K, Menezes LF, Garcia-Gonzalez MA, Huso DL, Germino GG: A critical developmental switch defines the kinetics of kidney cyst formation after loss of Pkd1. *Nat Med* 13: 1490–1495, 2007
17. Hayashi S, McMahon AP: Efficient recombination in diverse tissues by a tamoxifen-inducible form of Cre: A tool for temporally regulated gene activation/inactivation in the mouse. *Dev Biol* 244: 305–318, 2002
18. Wodarczyk C, Rowe I, Chiaravalli M, Pema M, Qian F, Boletta A: A novel mouse model reveals that polycystin-1 deficiency in ependyma and choroid plexus results in dysfunctional cilia and hydrocephalus. *PLoS One* 4: e7137, 2009
19. Karihaloo A, Koraishy F, Huen SC, Lee Y, Merrick D, Caplan MJ, Somlo S, Cantley LG: Macrophages promote cyst growth in polycystic kidney disease. *J Am Soc Nephrol* 22: 1809–1814, 2011
20. Ockuly JC, Gielissen JM, Levenick CV, Zeal C, Groble K, Munsey K, Sutula TP, Stafstrom CE: Behavioral, cognitive, and safety profile of 2-deoxy-2-glucose (2DG) in adult rats. *Epilepsy Res* 101: 246–252, 2012
21. Stafstrom CE, Roopra A, Sutula TP: Seizure suppression via glycolysis inhibition with 2-deoxy-D-glucose (2DG). *Epilepsia* 49[Suppl 8]: 97–100, 2008
22. Minor RK, Smith DL Jr., Sossong AM, Kaushik S, Poosala S, Spangler EL, Roth GS, Lane M, Allison DB, de Cabo R, Ingram DK, Mattison JA: Chronic ingestion of 2-deoxy-D-glucose induces cardiac vacuolization and increases mortality in rats. *Toxicol Appl Pharmacol* 243: 332–339, 2010
23. Wolfer DP, Lipp HP: A new computer program for detailed off-line analysis of swimming navigation in the Morris water maze. *J Neurosci Methods* 41: 65–74, 1992
24. Foxall PJ, Price RG, Jones JK, Neild GH, Thompson FD, Nicholson JK: High resolution proton magnetic resonance spectroscopy of cyst fluids from patients with polycystic kidney disease. *Biochim Biophys Acta* 1138: 305–314, 1992
25. Raez LE, Papadopoulos K, Ricart AD, Chiorean EG, Dipaola RS, Stein MN, Rocha Lima CM, Schlesselman JJ, Tolba K, Langmuir VK, Kroll S, Jung DT, Kurtoglu M, Rosenblatt J, Lampidis TJ: A phase I dose-escalation trial of 2-deoxy-D-glucose alone or combined with docetaxel in patients with advanced solid tumors. *Cancer Chemother Pharmacol* 71: 523–530, 2013

26. Stein M, Lin H, Jeyamohan C, Dvorzhinski D, Gounder M, Bray K, Eddy S, Goodin S, White E, Dipaola RS: Targeting tumor metabolism with 2-deoxyglucose in patients with castrate-resistant prostate cancer and advanced malignancies. *Prostate* 70: 1388–1394, 2010
27. Lin C, Wu H, Tjeerdema R, Viant M: Evaluation of metabolite extraction strategies from tissue samples using NMR metabolomics. *Metabolomics* 3: 55–67, 2007
28. Cobas C, Seoane F, Domínguez S, Sykora S, Davies AN: A new approach to improving automated analysis of proton NMR. *Spectrosc Eur* 23: 26–30, 2010
29. Fan TW, Lane AN, Higashi RM, Farag MA, Gao H, Bousamra M, Miller DM: Altered regulation of metabolic pathways in human lung cancer discerned by (13)C stable isotope-resolved metabolomics (SIRM). *Mol Cancer* 8: 41, 2009
30. Fan TW, Lane AN, Higashi RM, Yan J: Stable isotope resolved metabolomics of lung cancer in a SCID mouse model. *Metabolomics* 7: 257–269, 2011

This article contains supplemental material online at http://jasn.asnjournals.org/lookup/suppl/doi:10.1681/ASN.2015030231/-/DCSupplemental.

[a]Litter	[b]genotype	[c]phenotype	[d]treatment	[e]T=0 MRI TKV (cm^3)	[e]T=1M MRI TKV (cm^3)	[e]T=2M MRI TKV (cm^3)
A	*Pkd1*$^{\Delta C/flox}$	control	2DG	/	0.42	0.39
	Pkd1$^{\Delta C/flox}$: TmCre	cystic	NaCl	/	1.56	3.80
	Pkd1$^{\Delta C/flox}$: TmCre	cystic	2DG	/	1.32	2.58
B	*Pkd1*$^{flox/+}$: TmCre	control	NaCl	0.38	0.49	0.56
	Pkd1$^{\Delta C/flox}$	control	2DG	0.28	0.34	0.35
	Pkd1$^{\Delta C/flox}$: TmCre	cystic	NaCl	0.79	1.72	3.91
	Pkd1$^{\Delta C/flox}$: TmCre	cystic	2DG	0.61	1.21	3.23
C	*Pkd1*$^{flox/+}$	control	2DG	0.36	0.36	0.41
	Pkd1$^{\Delta C/flox}$: TmCre	cystic	NaCl	1.19	2.48	3.71
	Pkd1$^{\Delta C/flox}$: TmCre	cystic	NaCl	0.83	2.65	3.61
	Pkd1$^{\Delta C/flox}$: TmCre	cystic	2DG	1.19	2.24	3.70
	Pkd1$^{\Delta C/flox}$: TmCre	cystic	2DG	1.19	2.31	3.37
	Pkd1$^{\Delta C/flox}$: TmCre	cystic	2DG	0.60	1.10	2.27
	Pkd1$^{\Delta C/flox}$: TmCre	cystic	2DG	0.59	1.30	3.01
D	*Pkd1*$^{\Delta C/flox}$	control	NaCl	0.43	0.46	0.49
	Pkd1$^{\Delta C/flox}$	control	2DG	0.60	0.67	0.70
	Pkd1$^{flox/+}$	control	2DG	0.32	0.32	0.33
	Pkd1$^{\Delta C/flox}$: TmCre	cystic	NaCl	1.18	2.26	4.14
	Pkd1$^{\Delta C/flox}$: TmCre	cystic	NaCl	1.31	2.79	5.32
	Pkd1$^{\Delta C/flox}$: TmCre	cystic	2DG	1.02	1.46	2.24
	Pkd1$^{\Delta C/flox}$: TmCre	cystic	2DG	0.71	1.00	1.41
E	*Pkd1*$^{HA/+}$: TmCre	control	NaCl	0.42	0.47	0.48
	Pkd1$^{flox/+}$	control	2DG	0.37	0.38	0.42
	Pkd1$^{\Delta C/flox}$: TmCre	cystic	NaCl	0.91	1.92	3.78
	Pkd1$^{\Delta C/flox}$: TmCre	cystic	2DG	1.01	2.22	3.49

Supplementary Table 1. Measurements of kidney volume by MRI of each long-term animal model employed in the study. a. Animals are shown within the individual litters. 5 independent litters were employed for the studies divided in A to E; **b.** the precise genotype of each animal employed in the study is shown; **c.** the phenotype classified as control (non cystic) or cystic kidneys are indicated; **d.** the type of treatement 2-deoxy-D-glucose (2DG) or vehicle only (NaCl) is indicated; e. total kidney volumes were calculated in cm^3 at the different timepoints: T=0, prior to treatment T=1M and T=2M one and two months after treatment respectively are indicated for each animal.

Biochemical parameter	Wt NaCl mean ± SEM			Wt 2DG mean ± SEM		
	T=0 MRI P55	T=1M MRI P85	P130	T=0 MRI P55	T=1M MRI P85	P130
BUN	40.00 ± 5.72	42.57 ± 2.67	39.33 ± 3.09	34.90 ± 5.01	43.70 ± 2.72	42.86 ± 3.13
ALT	39.86 ± 6.50	41.86 ± 2.33	50.00 ± 15.13	42.70 ± 6.53	60.75 ± 8.53	81.25 ± 22.47
AST	92.43 ± 16.32	81.86 ± 13.12	126.50 ± 34.70	109.10 ± 13.96	105.60 ± 13.84	121.4 ± 8.05
LDH-P	768.30 ± 85.29	720.40 ± 113.60	726.20 ± 104.00	814.80 ± 78.37	753 ± 65.53	701.90 ± 79.24
ALB	2.93 ± 0.13	3.14 ± 0.092	3.27 ± 0.099	2.83 ± 0.094	2.93 ± 0.075	3.17 ± 0.100
CK	661.1 ± 241.3	401.3 ± 125.6	1036 ± 350.3	741.6 ± 177.1	323.3 ± 57.2	585.9 ± 143.0

Supplementary Table 2: Biochemical parameters at various timepoints after long-term 2DG treatment as compared to NaCl treatment. Blood Urea Nitrogen (BUN), alanine aminotransferase (ALT), aspartate aminotransferase (AST), lactate deshydrogenase-P (LDH-P), albumin (ALB) and creatine kinase (CK) were measured in the sera collected at P55, P85 and P130 from mice treated with vehicle or 2DG at 100 mg per Kg. Data are presented as Mean +/- SEM

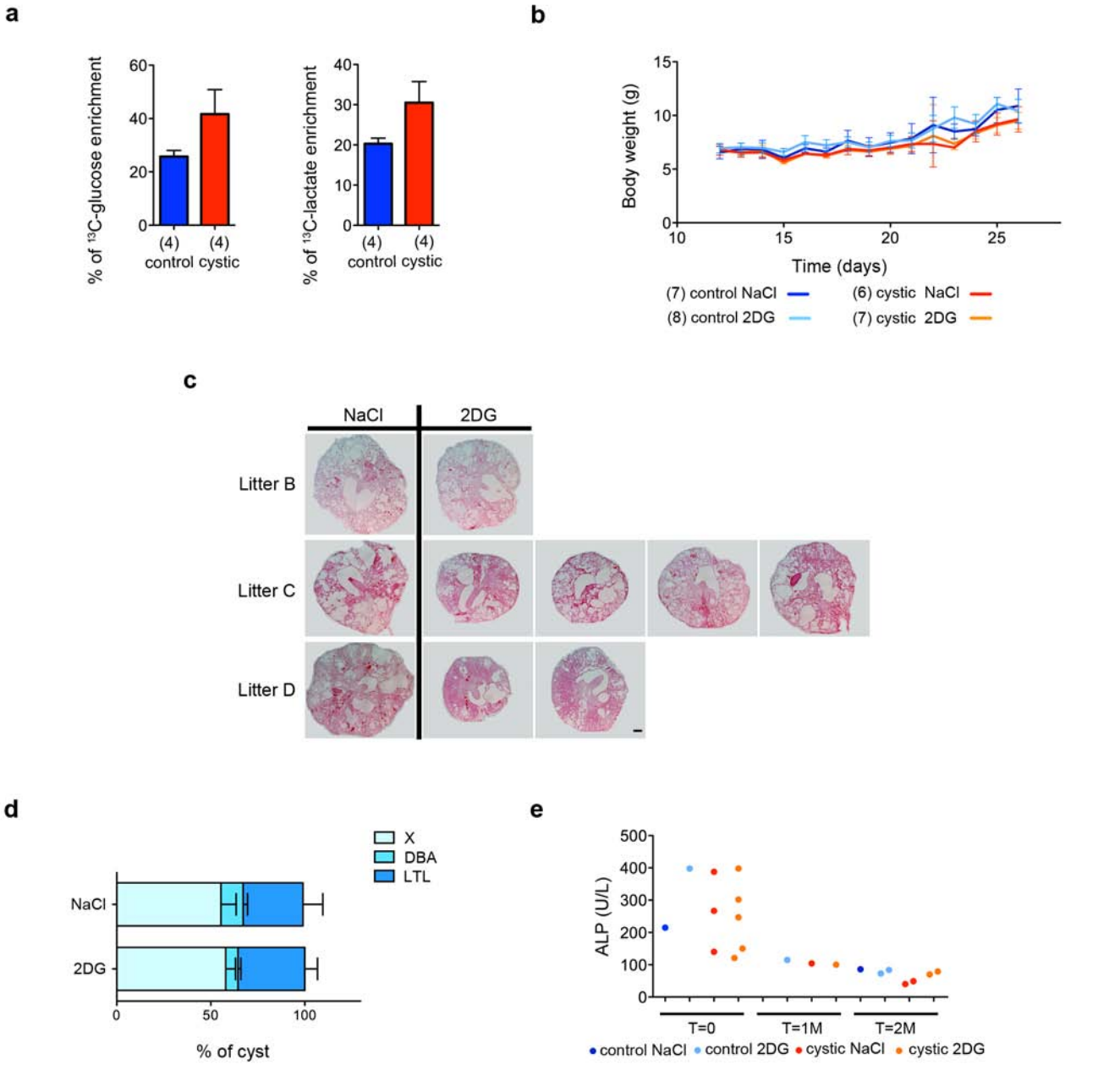

Chiaravalli et al, 2DG in PKD. Supplementary figure 1

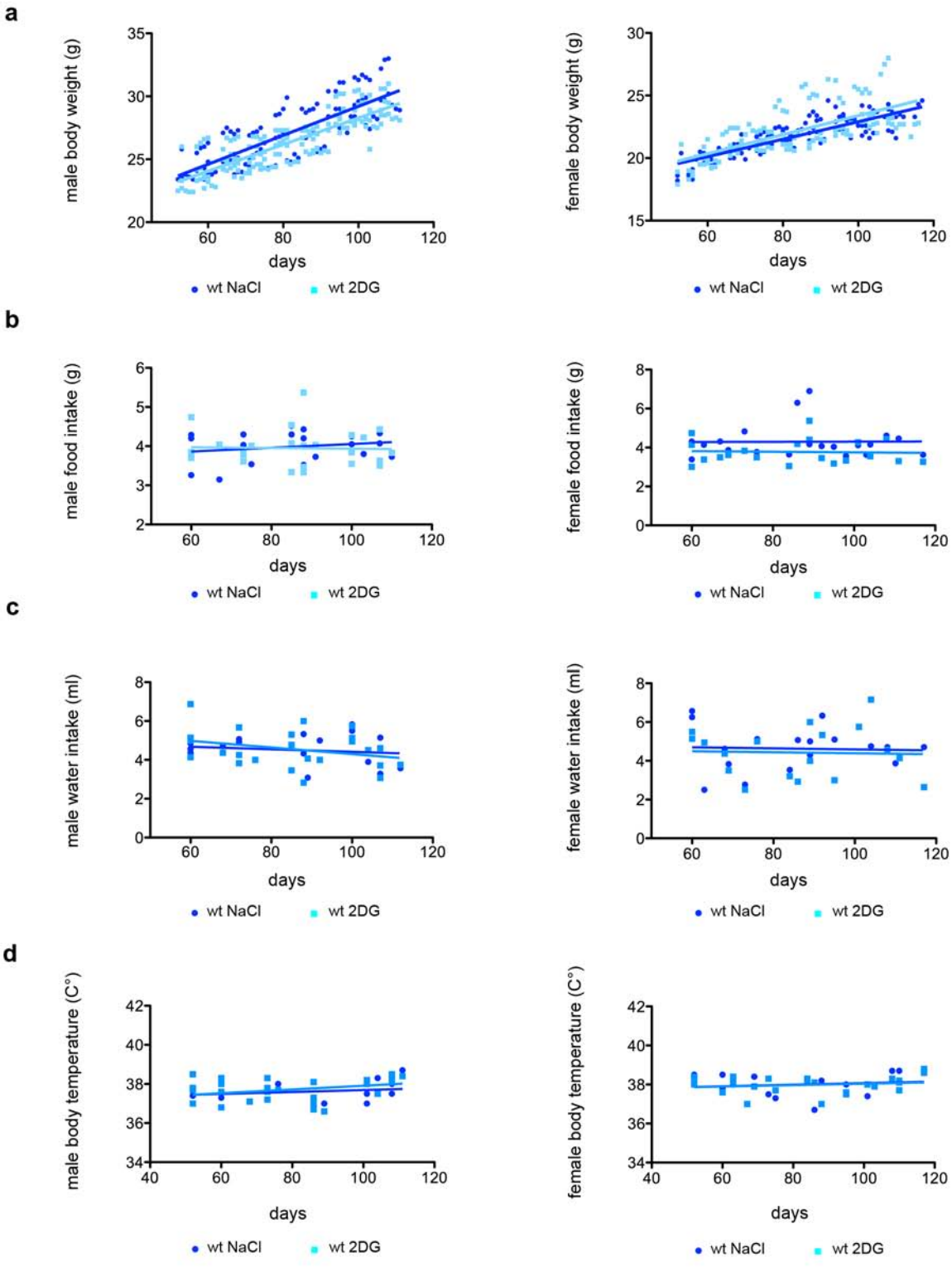

Chiaravalli et al, 2DG in PKD. Supplementary figure 2

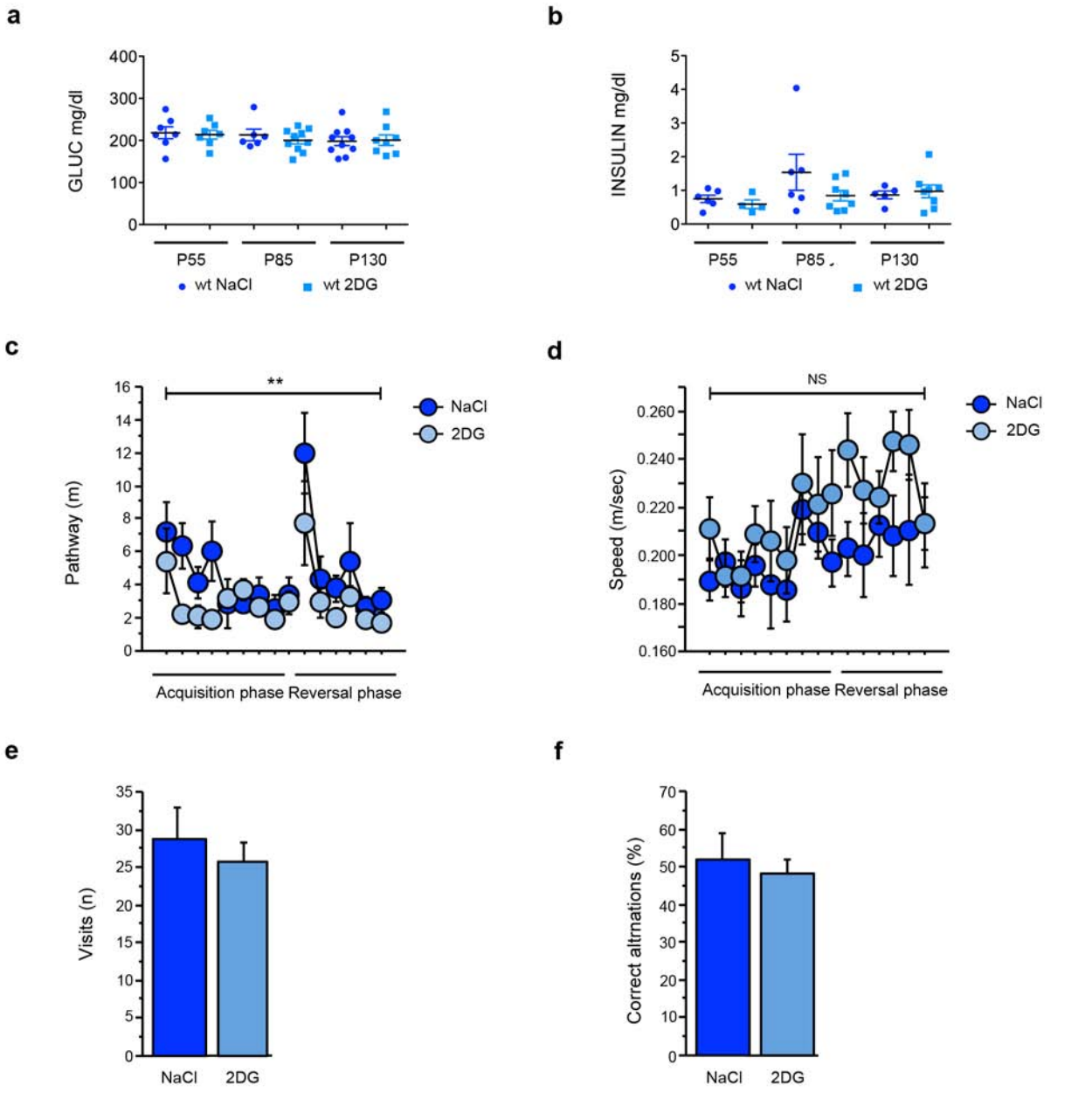

Chiaravalli et al, 2DG in PKD. Supplementary Figure 3

Supplementary Figure 1

a. The percentage of ^{13}C-glucose and ^{13}C-lactate enrichment (calculated as described in Materials and Methods) was higher in the kidneys from the cystic mice from the medium-term model as described in **Figure 1a**. **b**. Growth curve from mice treated with 2DG or vehicle during the medium-term-experiment. **c**. Histology of kidney sections from four litters collected from long term model treated with 2DG or vehicle. **d**. Percentage of cyst that stain positive for DBA, LTL or negative for both (X) in the long-term PKD model treated with NaCl or 2DG. No significant differences in the origin of cyst distribution could be observed, suggesting that 2DG acts equally on all cysts. **e**. Alkaline Phosphatase (ALP) concentration of the serum collected at the same time point of the first (T=0), second (T=1M) and third (T=2M) MRI (one, two and three months after tamoxifen induction) of the long term experiment.

Supplementary Figure 2: 2DG treatment has no systemic effects. Body weight (**a**), food intake (**b**), water intake (**c)** and body temperature (**d**) were not altered in males (left) and females (right) after treatment with 100 mg per kg 2DG 5 days a week for 2.5 months.

Supplementary Figure 3: 2DG treated mice show no differences in glucose and insulin levels and normal motor ability and working memory. a-b. Analysis of glucose (**a**) or insulin (**b**) levels at the different time points in mice treated with 2DG or NaCl show no differences in circulating insulin or glucose levels. **c.** Improved pathway to reach the platform in the 2DG treated versus NaCl treated animals in the Morris water maze test was observed (ANOVA repeated measures for pathway $F[1, 12]=9.7$, $p=0.0009$ with no interaction between treatment*days $F[1, 14]=0.9$, $p=0.5$). **d.** No differences were observed between groups during the water maze test in the speed ($F[1,12]=1.15$, $p=0.3$). **e-f.** Spontaneous alternation test was performed to assess short-term working memory. No differences between 2DG and vehicle treated mice were observed for the number of visits ($F[1,12]=0.4$, $p=0.53$) (**e**) and for the percentage of correct alternations ($F[1,12]=0.23$, $p=0.63$) (**f**). Data points and bars represent the mean +/- SEM in from **a** to **d**. Histograms represent the mean ± SEM in **e** and **f**.